Original Article

Association between quadriceps fat pad edema and patellofemoral osteoarthritis: a quantitative Q-Dixon-based magnetic resonance imaging (MRI) analysis

Liangjing Lyu[#]^, Jing Ren[#]^, Wenjie Lu^, Yongliang Li^, Jingyu Zhong^, Weiwu Yao^

Department of Radiology, Tongren Hospital, Shanghai Jiao Tong University School of Medicine, Shanghai, China

Contributions: (I) Conception and design: L Lyu; (II) Administrative support: W Yao; (III) Provision of study materials or patients: W Yao; (IV) Collection and assembly of data: J Ren, W Lu; (V) Data analysis and interpretation: L Lyu, J Zhong, Y Li; (VI) Manuscript writing: All authors; (VII) Final approval of manuscript: All authors.

[#]These authors contributed equally to this work.

Correspondence to: Jingyu Zhong, MD, PhD; Weiwu Yao, MD, PhD. Department of Radiology, Tongren Hospital, Shanghai Jiao Tong University School of Medicine, No. 1111 Xianxia Road, Shanghai 200336, China. Email: ZJY4623@shtrhospital.com; YWW4142@shtrhospital.com.

Background: Anterior knee pain (AKP) is a common symptom of patellofemoral osteoarthritis (PFOA). There is limited prospective evidence supporting the relationships between patellofemoral maltracking parameters, AKP, and PFOA. Thus, this prospective cross-sectional study aimed to determine the association between quadriceps fat pad (QFP) edema and patellofemoral maltracking in patients with chronic AKP and to evaluate the feasibility and diagnostic performance of a PFOA assessment using fat fraction (FF) and T2* based on Q-Dixon.

Methods: This was a cross-sectional study with prospective data collection. Patients with chronic AKP were recruited from an orthopedic outpatient magnetic resonance imaging (MRI) waiting room at Shanghai Tongren Hospital between November 1, 2022, and April, 30, 2023. Exclusion criteria included age of <18 years, knee trauma, major internal derangement, prior surgery/arthroscopy, pre-existing joint diseases, and contraindications to MRI. MRI was performed using a 3.0-T instrument, and patellofemoral maltracking parameters were measured. Patellofemoral feature-relevant items, including patellar cartilage defects, patellar bone marrow lesions (BMLs), patellar osteophytes, anterior femoral osteophytes, Hoffa synovitis, and synovitis-effusion, from the semi-quantitative MRI Osteoarthritis Knee Score (MOAKS) were measured. The Anterior Knee Pain Scale (AKPS) was used to assess pain and function. FF/T2* measurement differences between groups and their associations with maltracking metrics, osteoarthritis grading based on the Iwano grading system, MOAKS, and AKPS, were investigated. Based on Iwano grading, the participants were categorized as having no-PFOA (n=40), mild PFOA (n=40), and advanced PFOA (n=40). Chi-squared and one-way analysis of variance were used to assess potential differences between the groups. Spearman's correlation test was used to analyze the correlation between the morphological parameters, AKPS, Iwano grade, MOAKS, and MRI quantitative values. Receiver operating characteristic (ROC) curves assessed the area under the curve (AUC), sensitivity, and specificity of quantitative values for distinguishing PFOA from no-PFOA.

^ ORCID: Liangjing Lyu, 0000-0003-4643-9740; Jing Ren, 0009-0000-5330-5383; Wenjie Lu, 0009-0005-3714-2496; Yongliang Li, 0000-0002-5838-1227; Jingyu Zhong, 0000-0002-9817-2294; Weiwu Yao, 0000-0002-1536-9324.

Results: Among the 120 included patients, those in the mild (86.2±8.5) and advanced (83.9±9.5) PFOA groups had significantly lower AKPS scores than those in the no-PFOA group (88.8±7.3) (P=0.03). The mean FF and T2* values of the QFP were significantly higher in the no-PFOA group than those in the mild and advanced PFOA groups (P<0.001 for FF and P=0.02 for T2*). Quantitative data on the QFP and patellofemoral maltracking parameters showed no association. FF (r=–0.686, P<0.001) and T2* (r=–0.314, P=0.008) showed a negative correlation with the Iwano grade. The AUCs for PFOA diagnosis were 0.906 [95% confidence interval (CI), 0.853–0.960] (FF) and 0.744 (95% CI, 0.657–0.831) (T2*).

Conclusions: QFP FF and T2* were not associated with patellofemoral maltracking parameters but with increased PFOA in patients with AKP, suggesting that QFP abnormalities play a role in PFOA. Therefore, a quantitative QFP assessment (FF and T2*) based on Q-Dixon technology could be a convenient and reliable new imaging biomarker for PFOA severity during clinical diagnosis, treatment, and follow-up.

Keywords: Knee osteoarthritis; patellofemoral joint; magnetic resonance imaging (MRI); fat pad; edema

Submitted Dec 05, 2023. Accepted for publication Mar 20, 2024. Published online Apr 17, 2024.
doi: 10.21037/qims-23-1730
View this article at: https://dx.doi.org/10.21037/qims-23-1730

Introduction

Anterior knee pain (AKP) is a typical symptom of patellofemoral (PF) osteoarthritis (OA) (PFOA) (1). The PF joint is usually affected first by knee OA (KOA) but receives less attention than the tibiofemoral joint (TFJ) (2). While PFOA can develop at any age (3), 24% of adults aged 26–50 years and 55% of adults aged 40–50 years have PFOA based on radiographic findings (4). Hence, 40–50% of patients with AKP have PFOA (5,6). PF maltracking increases the likelihood of developing PFOA. However, prospective studies (7) have provided limited evidence on the relationships between PF maltracking parameters, AKP, and PFOA.

Peripatellar fat pads, including the infrapatellar fat pad (IFP), quadriceps fat pad (QFP), and prefemoral fat pad, play important roles in biomechanics (8) and secretion action (9). Recurrent impingement, friction, trauma, or knee joint instability cause peripatellar fat pad edema, leading to alterations (10) in the biomechanical and biochemical mechanisms. As a result, cytokine and synovial fluid production are affected, potentially leading to KOA progression. Recent studies (11,12) have confirmed the relationship between IFP edema (IFPE) and PF maltracking parameters. However, only a few studies have focused on the highly prevalent (12–14%) QFP edema (QFPE) (13,14). The QFP assessment parameters for investigating KOA include the mass effect, morphological measurements, and altered signal intensity (10,15,16). However, a direct and convenient method for quantitative QFP assessment, with improved objectivity and repeatability, is currently lacking. Q-Dixon, a mature and reliable quantitative technique, is used in clinical practice to measure fatty liver (17). A single fast scan provides multiple quantitative images, such as fat fraction (FF) and T2* maps, which allow direct measurement. Chen *et al.* (18) quantified IFP with FF/T2* and demonstrated their use as new imaging biomarkers for KOA assessment. We quantified QFP using a similar sequence and assessed its potential as an alternative imaging biomarker for PFOA, particularly in IFP cases with direct trauma, cyclops lesions, and tumors.

In this study, we aimed to confirm the relationship between QFP and maltracking parameters in patients with AKP. We also assessed the feasibility and diagnostic performance of FF and T2* values in identifying QFP pathological variations in PFOA. We present this article in accordance with the STROBE reporting checklist (available at https://qims.amegroups.com/article/view/10.21037/qims-23-1730/rc).

Methods

Study population

Ethical approval for this cross-sectional study with prospective data collection was obtained from the Institutional Review Board of Shanghai Tongren Hospital, and informed consent was obtained from the participants. The research reported in this article adhered to the guidelines of the Declaration of Helsinki (as revised in 2013).

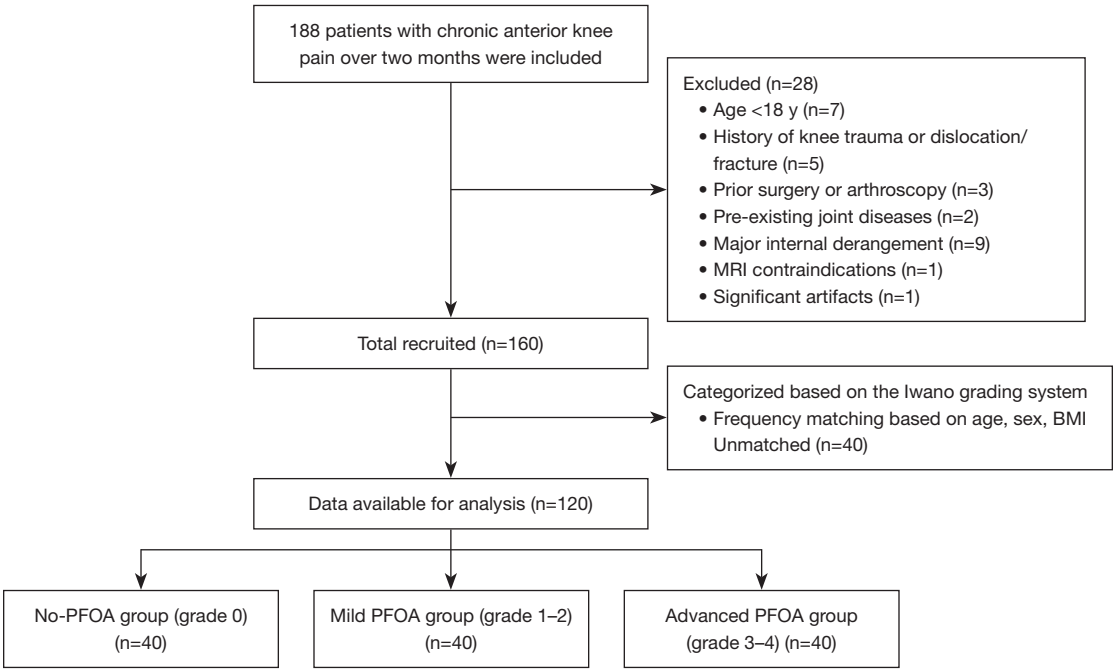

Figure 1 Flowchart depicting study population selection. y, years; MRI, magnetic resonance imaging; BMI, body mass index; PFOA, patellofemoral osteoarthritis.

The study population included 188 consecutive patients [age 50.13±13.34 years; 96 (51.06%) women] with AKP. All patients were recruited from the orthopedic outpatient MRI waiting room between November 1, 2022, and April 30, 2023. The inclusion criterion was a history of AKP, defined as pain around the patella for over two months and confirmed by an orthopedic outpatient surgeon. The exclusion criteria were age <18 years, history of knee trauma or dislocation/fracture, major internal derangement (torn meniscus, tendon, or cruciate ligament), prior surgery or arthroscopy, pre-existing joint diseases (tumors or tumor-like diseases, autoimmune rheumatic disease, or metabolic disorders), and absolute or relative contraindications to magnetic resonance imaging (MRI). Images with significant artifacts were excluded from the analysis. According to the International Physical Activity Questionnaire (IPAQ) short form (score: 1–3) (19), each participant's physical activity was classified as low, moderate, or high. All participants underwent radiography and MRI of the knee joint and were graded based on the Iwano grading system, a radiographic (skyline views) classification system specifically developed for PFOA assessment (20). This system grades PFOA as follows: grade 0, normal PF joint space; grade 1, mildly narrowed PF joint space (≥3 mm); grade 2, moderately narrowed PF joint space (<3 mm) and free of bone contact; grade 3, PF joint bone contact less than one-quarter of the articular surfaces; and grade 4, PF joint bone contact (greater than one-quarter of the articular surfaces). Based on the PFOA assessment, the study participants were categorized as having no PFOA (grade 0), mild PFOA (grades 1–2), or advanced PFOA (grades 3–4). To control for the effects of individual physiological factors, we performed frequency matching based on age, sex, and body mass index (BMI). Hence, we included three groups, with 40 knees in each group (*Figure 1*). Sample size estimates are shown in the Appendix 1.

AKP assessment

Pain and knee function were assessed using the Anterior Knee Pain Scale (AKPS) (21,22). All participants completed the AKPS questionnaire survey, comprising 13 questions evaluated on a scale of 0–100, with lower scores indicating worse knee pain and disability (23).

Radiographic assessment

All participants underwent radiography of the target knee in the standing anteroposterior, lateral, and skyline views. Two

Table 1 Magnetic resonance imaging parameters

Parameters	T1W	PDW	PDW	T2W	Liver Lab
Acquisition	Coronal	Sagittal	Coronal	Transverse	Sagittal
Repetition time (ms)	363	2,240	2,350	3,570	9
Echo time (ms)	12	30	30	58	1.05, 2.46, 3.69, 4.92, 6.15, 7.38
Flip angle (°)	90	150	150	150	4
Section thickness (mm)	3	3	3	3	0.9
Voxel resolution (mm)	0.4×0.4×3.0	0.5×0.5×3.0	0.5×0.5×3.0	0.4×0.4×3.0	1.2×1.2×1.2
Field of view	160	160	160	160	230
Average	1	1	1	1	3
Scan time (s)	68	87	91	82	35

T1W, T1-weighted; PDW, proton density-weighted; T2W, T2-weighted.

musculoskeletal radiologists assessed the images and reached a consensus based on Iwano grading (grades 0–4) (20).

MRI protocol

MRI was performed on the target knee using a Siemens MAGNETOM Vida 3.0-T scanner (Siemens Healthineers, Erlangen, Germany) with an 18-channel knee coil. All the patients were examined in the supine position with mild knee flexion (15°–20°). Several MRI-safe cotton cushions were used to ensure patient comfort during the analysis. Conventional T1-weighted (T1W), T2-weighted turbo spin-echo fat suppression (T2W-TSE-FS), and proton density-weighted turbo spin-echo fat suppression (PDW-TSE-FS) sequences were obtained for the initial evaluation. For FF and T2* quantification, a multi-echo Q-Dixon volumetric interpolated breath-hold examination (VIBE) (Liver Lab) sequence was used. The sequence parameters are listed in *Table 1*.

Assessment of MRI knee morphology

Two musculoskeletal radiologists independently measured the sagittal and transverse T2W images for maltracking parameters, including the tibial tubercle-trochlear groove distance (TT-TG), lateral trochlear inclination (LTI), modified Insall-Salvati ratio (MISR), and patellar tilt angle (PTA). The medial and lateral facets were assessed based on the Wiberg classification as follows (24): type I, medial/lateral facets were roughly equal; type II, medial facet was relatively smaller than the lateral facet; and type III, medial facet was obviously smaller than the lateral facet. Details of morphological measurements are presented in *Figure 2*.

Semi-quantitative scoring of MRI scans

Sagittal/coronal PDW, transverse T2W, and sagittal T1W images were assessed by a musculoskeletal radiologist with two years of experience using the semi-quantitative MRI Osteoarthritis Knee Score (MOAKS) (25) and confirmed by musculoskeletal radiologists with ten years of experience. As the MOAKS was designed to assess evidence of OA in an older population and contains femorotibial features less associated with AKP, we chose the most relevant and common components for a complete PF feature evaluation (26,27). The following items were scored: (I) patellar cartilage defects (0–6) (the size of cartilage loss in the medial and lateral patellar subregion scores were combined for a score of 0–6), (II) patellar bone marrow lesions (BMLs) (0–6) (the volume of BMLs in the medial and lateral patellar subregion scores were combined for a score of 0–6), (III) patellar osteophytes (0–3), (IV) anterior femoral osteophytes (0–3), (V) Hoffa synovitis (0–3), and (VI) synovitis-effusion (0–3).

Quantitative assessment of QFP

FF and T2* maps were acquired using a multi-echo Q-Dixon VIBE (Liver Lab) sequence. The QFPs were segmented manually on the FF images using ITK-SNAP version 3.6.0 within the middle five slices (with the slice passing through the patellar ridge defined as the central slice) on sagittal FF mapping images, avoiding the quadriceps tendon,

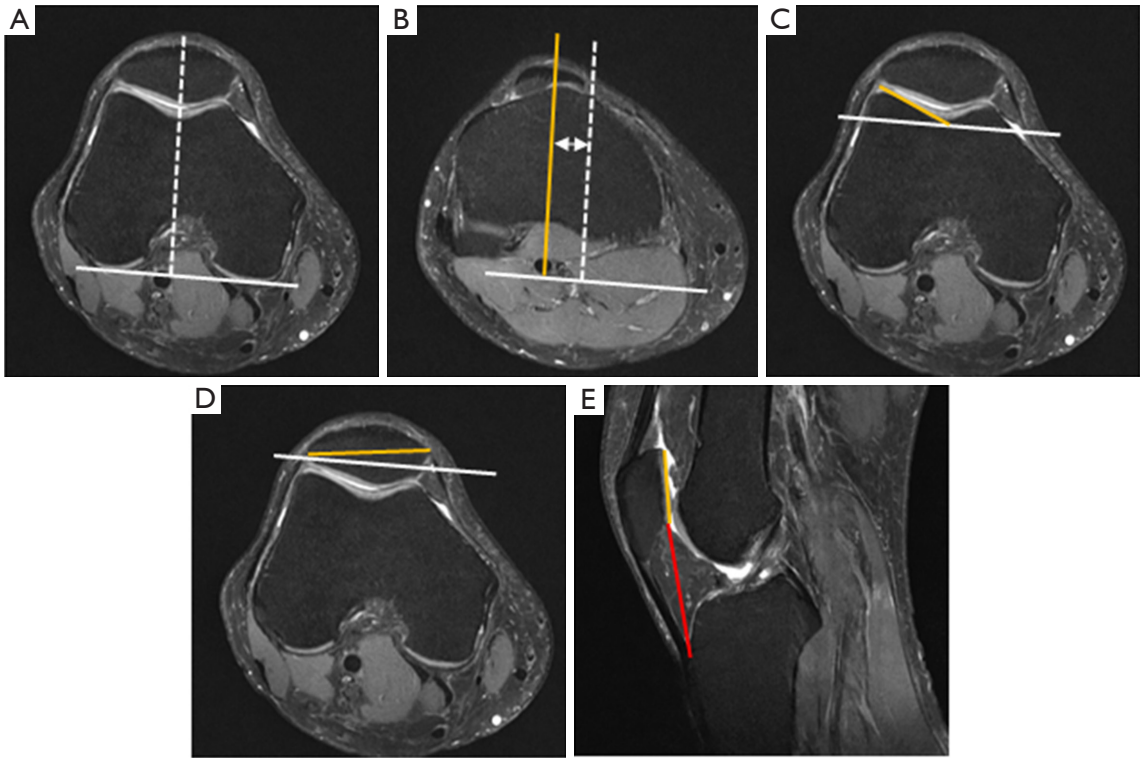

Figure 2 Assessment of patellofemoral maltracking. (A) A white baseline is drawn on the slice at the most posterior position of the femoral condyles. The vertical white dashed line is placed through the deepest point of the TG. (B) The lines in (A) are then transferred to the slice of the patellar tendon attachment to the TT. The vertical yellow line passes through the central point of the attachment. The TT-TG distance is indicated by the double-headed arrow. (C) The angle between the white baseline and the yellow line, along with the subchondral bone facet of the lateral trochlear, represents the LTI. (D) The angle between the yellow patellar widest line and the white baseline represents the PTA. (E) The modified Insall-Salvati ratio is between the red line (distance from the inferior patellar cartilage pole to the TT) and the yellow line (the vertical diameter of the patellar cartilage). TG, trochlear groove; TT, tibial tubercle; LTI, lateral trochlear inclination; PTA, patellar tilt angle.

suprapatellar bursa, and patella. The target segments were drawn synchronously and automatically on the T2* mapping images because the T2* and FF mapping images were obtained from the same Q-Dixon VIBE sequences, indicating that they were equivalent to the registration images. Two radiologists independently performed the segmentations and calculated the quantitative data (FF and T2* values) to assess inter- and intra-observer reliabilities. The quantitative results for each knee were averaged from the values calculated from the five slices and recorded as the average of the values from the two observers.

Statistical analysis

IBM SPSS Statistics for Windows, version 23.0 (IBM Corp., USA), was used for statistical analysis, with two-sided $P<0.05$ indicating significance. Continuous data were reported as means and standard deviations, while categorical data were reported as frequencies and percentages. The missing data were addressed by the Mean/Mode Completer. The Shapiro-Wilk test was utilized for the normality test. The intraclass correlation coefficient was used to access inter- or intra-observer reliability and graded (28) as poor (<0.500), moderate (0.500–0.750), good (0.751–0.900), or excellent (>0.900). Chi-squared (dichotomous variables) and one-way analysis of variance, followed by Bonferroni's post hoc multiple comparison (continuous variables) tests, were used to assess potential differences between the groups. Spearman's correlation test analyzed the correlation between the morphological parameters, AKPS, Iwano grade, MOAKS, and MRI quantitative values. Correlation coefficient (r) values were used to categorize correlations

Table 2 Clinical characteristics

Variable	No-PFOA (n=40)	Mild PFOA (n=40)	Advanced PFOA (n=40)	P value
Gender (female)	21 (52.5)	23 (57.5)	24 (60.0)	0.40*
Age (years)	48.9±7.2	52.5±4.9	53.8±3.2	0.28
BMI (kg/m^2)	24.5±3.2	23.9±2.9	24.8±2.4	0.68
IPAQ	1.8±0.2	1.7±0.7	1.5±0.3	0.17
AKPS	88.8±7.3	86.2±8.5	83.9±9.5	0.03
Wiberg classification	N/A	N/A	N/A	N/A
Type				0.46*
I	19 (47.5)	18 (45.0)	18 (45.0)	
II	17 (42.5)	19 (47.5)	14 (35.0)	
III	4 (10.0)	3 (7.5)	8 (20.0)	
Iwano				
0	40	N/A	N/A	N/A
1	N/A	28	N/A	N/A
2	N/A	12	N/A	N/A
3	N/A	N/A	33	N/A
4	N/A	N/A	7	N/A

Data are presented as means ± standard deviations or frequencies and percentages in parentheses. *, statistic of the Pearson Chi-squared test. PFOA, patellofemoral osteoarthritis; BMI, body mass index; IPAQ, International Physical Activity Questionnaire; AKPS, Anterior Knee Pain Scale; N/A, not applicable.

as mild (r=0.200–0.400), moderate (r=0.401–0.600), strong (r=0.601–0.800), or extremely strong (r>0.800). Receiver operating characteristic (ROC) curves calculated the area under the curve (AUC), sensitivity, and specificity of quantitative values for distinguishing PFOA from no-PFOA using Iwano grading as a reference.

Results

Patients

The included 120 knees without missing data were divided into three groups: no-PFOA (n=40), mild PFOA (n=40), and advanced PFOA (n=40) (*Figure 1*). *Table 2* summarizes the basic patient information, including age, sex, BMI, IPAQ, Wiberg classification, and AKPS scores. The groups showed no significant differences in age, sex, BMI, IPAQ, or Wiberg classification (P>0.05). The patients in the mild (86.2±8.5) and advanced (83.9±9.5) PFOA groups had significantly lower AKPS scores, indicating worse pain and disability, than those in the no-PFOA group (88.8±7.3) (P=0.03).

Inter- and intra-observer reproducibility for maltracking parameters and quantitative data

In the intra- and inter-observer reliability evaluations, TT-TG (0.958/0.923), MISR (0.970/0.954), PTA (0.946/0.928), FF (0.892/0.828), and T2* (0.807/0.761) showed good to excellent reliability, and LTI showed good reliability (0.885/0.850) (*Table 3*).

FF and T2 values in the no-PFOA and PFOA groups*

The QFP demonstrated significantly higher mean FF and T2* values in the no-PFOA group than those in the mild and advanced PFOA groups (FF, P<0.001; T2*, P=0.02) (*Table 4*; *Figures 3*,*4*).

Correlation between MRI quantitative data and maltracking parameters, OA clinic assessment, and MOAKS

The QFP quantitative data and PF maltracking parameters

Table 3 Assessment of intra- and inter-observer agreement

Variable	Intra-observer				Inter-observer			
	ICC	Lower	Upper	P value	ICC	Lower	Upper	P value
TT-TG	0.958	0.918	0.979	<0.001	0.923	0.851	0.960	<0.001
LTI	0.885	0.783	0.941	<0.001	0.850	0.720	0.922	<0.001
MISR	0.970	0.938	0.986	<0.001	0.954	0.849	0.983	<0.001
PTA	0.946	0.896	0.973	<0.001	0.928	0.861	0.963	<0.001
FF	0.892	0.735	0.956	<0.001	0.828	0.673	0.913	<0.001
T2*	0.807	0.523	0.922	<0.001	0.761	0.736	0.891	<0.001

ICC, Intraclass correlation coefficient; TT-TG, tibial tubercle-trochlear groove distance; LTI, lateral trochlear inclination; MISR, modified Insall-Salvati ratio; PTA, patellar tilt angle; FF, fat fraction.

Table 4 Comparison of quantitative data between groups

Parameter	No-PFOA (n=40)	Mild PFOA (n=40)	Advanced PFOA (n=40)	P value*
FF (%)	56.34±10.19	42.87±12.19	37.13±11.06	<0.001
T2* (ms)	12.68±5.08	10.86±3.65	10.17±2.02	0.02

Data are presented as means ± standard deviations. *P, statistic of the one-way analysis of variance test between the groups. PFOA, patellofemoral osteoarthritis; FF, fat fraction.

showed no associations, while FF alterations and AKPS showed a mild correlation (r=0.396, P=0.001) (*Table 5*). FF alterations showed a strong negative correlation with Iwano grading (r=–0.686, P<0.001), while T2* alterations showed a mild negative correlation (r=–0.314, P=0.008) (*Table 5*). *Table 5* shows the associations between the QFP quantitative data and MOAKS. The FF and T2* values were negatively correlated with patellar cartilage defects, patellar osteophytes, and anterior femoral osteophytes (r=–0.456, –0.630, and –0.440, respectively, for FF; and r=–0.253, –0.242, and –0.256, respectively, for T2*; P<0.05). FF was negatively correlated with patellar BML, Hoffa synovitis, and effusion (r=–0.376, –0.447, and –0.325, respectively; P<0.05).

Diagnostic abilities of FF and T2 values in PFOA*

The diagnostic performances of FF and T2* for PFOA were assessed using ROC curves (*Figure 5*). FF showed a sensitivity of 0.851 and specificity of 0.860 for PFOA diagnosis, with an AUC of 0.906 [95% confidence interval (CI), 0.853–0.960]. T2* showed a sensitivity of 0.703 and specificity of 0.729, with an AUC of 0.744 (95% CI, 0.657–0.831).

Discussion

Our findings revealed a relationship between QFP and maltracking parameters in patients with AKP and a strong negative correlation between QFP-related FF or T2* alterations and PFOA grade.

Consistent with previous findings (29), we found that PFOA mainly affects women. Although the underlying causes remain unclear, the possible reasons include thinner cartilage, higher levels of inflammatory biomarkers, and a higher incidence of obesity in women. AKP is associated with reduced function and a poor quality of life. PFOA is a common cause of AKP and is often the initial compartment affected in early-stage KOA, with subsequent involvement of the TFJ (30). Macri *et al.* (30) demonstrated that PFOA features, rather than TFOA features, were associated with AKP, congruent with our findings. Most studies related to OA have assessed knee pain using generalized knee pain, such as the Western Ontario and McMaster Osteoarthritis Index, as an outcome (30,31). Since this outcome might mask the actual cause of AKP in PFOA, we used the AKPS instead. However, the association between QFPE and AKP remains unclear. Roth *et al.* (32) reported a relationship

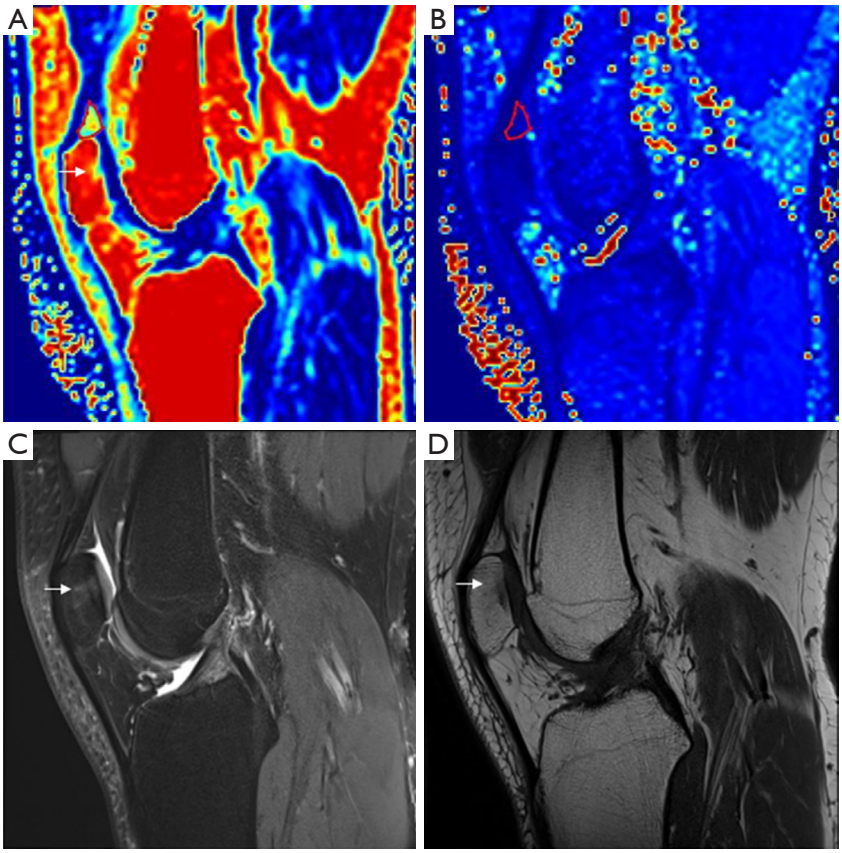

Figure 3 Measurements of FF and T2* maps in a 50-year-old woman with Iwano grade 0. The ROIs are drawn (red line) on FF maps (A) following the contour of the QFP and (B) simultaneously on the T2* maps. The FF and T2* were 51.86% and 15.22 ms, respectively. (A) FF maps, (C) proton density-weighted images, and (D) T1-weighted images show mild patellar edema (arrows). FF, fat fraction; ROIs, regions of interest; QFP, quadriceps fat pad.

between the QFPE and AKP, while Tsavalas (14) did not. Our results indicated a weak correlation between the FF of QFP and AKPS and no correlation between the T2* value of QFP and AKPS. We found that some AKP cases lacked QFPE and other abnormalities. This may be because non-mechanical features such as psychological factors and neurobiological alterations in pain signaling may also contribute to PFOA pain and dysfunction (33). In a study on QFPE, Yasemin *et al.* (15) reported vasculitis with obliteration of small vessels and complete relief from AKP after QFP resection. In another study on QFPE, Sirvanci *et al.* (34) reported myxoid degeneration and inflammation, and complete relief from AKP after steroid injection. Therefore, QFPE is not an incidental imaging finding; rather, it might be related to previous, ongoing, or potential AKP and warrants further evaluation in longitudinal studies. QFP syndrome is a clinical entity, and its diagnosis should be based on QFPE and AKP.

PF morphology measurements and QFP

During flexion and extension movements of the knee joint, the QFP prevents the quadriceps tendon and femoral condyle from touching, thereby improving PF engagement of the extensor mechanism. Abnormal PF morphology may contribute to maltracking and increase PF articular surface stress beyond tissue capacity. This may lead to the initiation or perpetuation of early PFOA, especially in young and physically active people with AKP (4). Other risk factors, including frequently descending stairs or squatting and quadriceps weakness, may also contribute to the development of PFOA (5). Radiological features of PFOA have been reported (4) in a quarter of young and middle-aged patients with AKP. IFPE is related to several

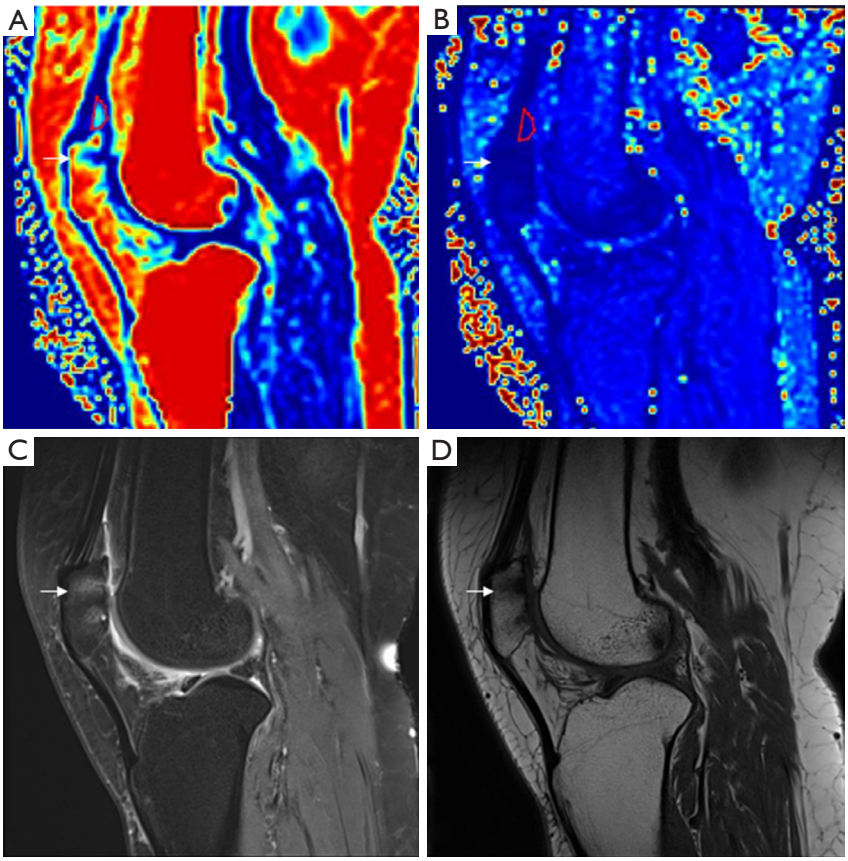

Figure 4 Measurements of FF and T2* maps in a 51-year-old woman with Iwano grade 3. The ROIs are drawn (red line) on FF maps (A) following the contour of the QFP and (B) simultaneously on the T2* maps. The FF and T2* were 21.76% and 8.71 ms, respectively. (A) FF maps, (B) T2* maps, (C) proton density-weighted images, and (D) T1-weighted images show severe patellar edema (arrows) with articular surface wear. FF, fat fraction; ROIs, regions of interest; QFP, quadriceps fat pad.

PF maltracking parameters, including the TT-TG, LTI, and PTA, especially the ISR or MISR, which indicate the patella alta (11,35). We used MISR instead of ISR to avoid the influence of patellar morphology (36,37). IFPE may be caused by PF maltracking, which triggers OA progression (38). QFPE, unlike IFP, was unrelated to the PF morphology measurements, which is consistent with the findings of Yuksel *et al.* (16) and Cosentino *et al.* (39). Although Yuksel *et al.* also included patients with AKP, only young adults (aged <40 years) were included. Cosentino *et al.* (39) suggested that QFPE might be a normal variant and did not overestimate its pathogenic significance. However, their participants were asymptomatic, while we focused on the AKP population. Hence, longitudinal studies are required to confirm the pathogenic significance of QFPE. Our findings showed a negative correlation between the FF of QFP and Hoffa's synovitis, indicating that, as active joint tissues, QFP and IFP can modulate inflammatory and destructive responses in KOA (9,10). Owing to this biochemical effect, QFPE has better potential for reflecting KOA severity than IFPE without PF maltracking interference. Further histological and pathological studies are necessary to validate these findings.

MOAKS and PFOA

The FF or T2* alteration from the QFP negatively correlated with several MOAKS features representing PFOA. Mechanical and biological dysfunctions of the knee joint can lead to OA. Although the specific OA pathomechanism is unclear, the medial compartment demonstrates a higher incidence or grade of KOA (30,40),

Table 5 Correlations between magnetic resonance imaging quantitative data and maltracking parameters, osteoarthritis clinic assessment, and MRI Osteoarthritis Knee Score

Variable	P* value (r)	P** value (r)
Maltracking parameters		
TT-TG	0.27 (N/A)	0.84 (N/A)
LTI	0.90 (N/A)	0.26 (N/A)
MISR	0.45 (N/A)	0.44 (N/A)
PTA	0.47 (N/A)	0.37 (N/A)
OA		
AKPS	0.001 (0.396)	0.63 (N/A)
Iwano grading	<0.001 (–0.686)	0.008 (–0.314)
Patella		
Cartilage defects	<0.001 (–0.456)	0.034 (–0.253)
BMLs	0.001 (–0.376)	0.54 (N/A)
Osteophytes		
Patella	<0.001 (–0.630)	0.044 (–0.242)
Femur anterior	<0.001 (–0.440)	0.033 (–0.256)
Synovitis		
Hoffa	<0.001 (–0.447)	0.47 (N/A)
Effusion	0.006 (–0.325)	0.29 (N/A)

*, statistic of the Spearman test between fat fraction and parameters; **, statistic of the Spearman test between T2* value and parameters. MRI, magnetic resonance imaging; TT-TG, tibial tubercle-trochlear groove distance; LTI, lateral trochlear inclination; MISR, modified Insall-Salvati ratio; PTA, patellar tilt angle; OA, osteoarthritis; AKPS, Anterior Knee Pain Scale; BMLs, bone marrow lesions; N/A, not applicable.

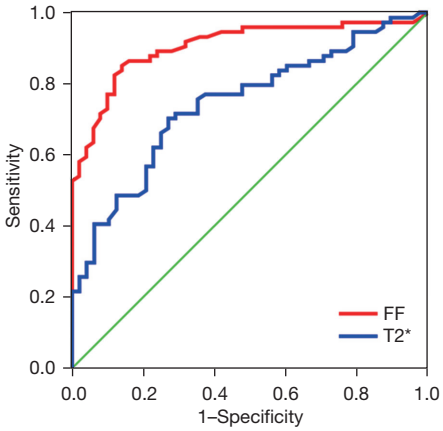

Figure 5 Diagnostic ability of FF and T2* values to identify PFOA. The ROC curves of FF and T2* values are used to assess the diagnostic ability. For discriminating between no-PFOA and PFOA, the AUC is 0.906 (95% CI, 0.853–0.960) for FF and 0.744 (95% CI, 0.657–0.831) for T2*. FF, fat fraction; PFOA, patellofemoral osteoarthritis; ROC, receiver operating characteristic; AUC, area under the curve; CI, confidence interval.

possibly because of the different mechanical forces on the medial and lateral compartments owing to joint instability and/or restriction. The medial compartment is typically the most load-bearing part. However, PFOA development differs in patients with AKP because the PF joint is not load-bearing. Among the available semi-quantitative scoring methods (25,41), the whole organ magnetic resonance imaging score (WORMS) is the most widely used. It simultaneously assesses cartilage defects for surface and thickness with a single scale score, making estimation challenging and non-ordinal in complex cases. In contrast, MOAKS enhances this score by providing two separate ordinal scores (0–3 per scale, total scale of 0–6) for cartilage defects (surface and thickness). Unlike WORMS, MOAKS simplifies the estimation by modifying BML size thresholds and scoring the entire subregion. Hence, we chose MOAKS over WORMS to evaluatePF features.

We found that cartilage defects, osteophytes, patellar BML, Hoffa's synovitis, and articular effusion were associated with FF or/and T2* alterations in the QFP. Although their causal relationship remains unknown, QFPE has a secretion effect (10) and is unrelated to any PF maltracking parameter in most studies (39,42). QFPE may occur before or concurrently with patellar structural abnormalities. Hence, the detection of QFPE may serve as a marker for simultaneous cartilage defects, BMLs, and osteophytes of the patella.

FF or T2 from QFP and OA*

Roth *et al.* proposed three theories of QFPE (32): (I) abnormal biomechanics and related impingement; (II) overuse injury or repetitive hyperflexion; and (III) reactive inflammation. Our results suggest that reactive inflammation is the most likely pathogenesis. Fontanella *et al.* (43) suggested that IFP is related to KOA, while QFP is unrelated. However, the authors only assessed QFP using volume and two dimensions on conventional MRI sequences rather than its internal signal. We propose that peripatellar

fat pads should be considered as having similar active adipose tissues, akin to the suprapatellar and IFPs, with potential involvement in KOA and association with cases exhibiting edema or effusion. We found that QFPE was closely related to PFOA severity. The alteration of internal signals can be quantified using FF and T2* relaxation. FF represents the percentage of pure fat content in tissue, reflecting internal pathological changes (18). Pathological processes such as edema, inflammatory responses, myxoid degeneration, vasculitis, and fibrosis in the QFP, similar to IFP pathogenesis, may increase the water content and decrease the fat content, resulting in decreased FF. Since water has a shorter T2* relaxation time than fat (40), the T2* value in QFP decreases as KOA develops. Moreover, fibrosis and vascularization may also reduce T2* relaxation in QFP. Our findings showed significant differences in FF and T2* between the mild, advanced, and no-PFOA groups (*Table 4*), consistent with the pathological course of KOA. Although Kellgren-Lawrence grading (KLG) is the most common classification of KOA, it is based on TFJ radiographic features and does not assess the PF joint. For patients with AKP and PFOA, Iwano grading may be more appropriate than KLG. We found a strong negative correlation between FF alteration of the QFP and Iwano grading. The ROC analysis demonstrated that FF had good accuracy in diagnosing PFOA, with an AUC of 0.906 (95% CI, 0.853–0.960). In contrast, the T2* value performed poorer than FF in diagnosing PFOA, possibly due to its susceptibility to magnetic field homogeneity. Therefore, a quantitative QFP based on Q-Dixon technology could be an effective and reliable new imaging biomarker for PFOA severity.

Our study has several limitations. Selection bias was unavoidable because of the limited sample size in this single-center study. Future studies with larger sample sizes covering larger populations are needed. We did not include patients with obvious internal derangement to reduce interference by other confounders; however, mild unascertained pathology may have influenced the results (we could not request every patient to undergo arthroscopy). Although we quantified QFPE, pathological biopsy remains challenging; thus, the exact pathological changes remain unknown. Prospective studies supported by histopathological data will help us gain a better understanding of the role of QFP in AKP. In addition, in some cases with normal MRI findings, we could not explain the exact cause of AKP, although we assume that psychological or neurological causes may play a role.

Conclusions

To our knowledge, this is the first study to use FF and T2* to quantitatively determine whether QFP abnormalities are associated with PF maltracking or PFOA development. Both FF and T2* values of QFP were not correlated with PF maltracking parameters but were associated with increased PFOA in patients with AKP, suggesting that QFP abnormalities play a role in PFOA. Therefore, FF and T2* of the QFP may be reliable tools for assessing PFOA severity. In addition, the QFP measurement is easier than the IFP measurement because of its smaller size and sharper definition.

Acknowledgments

We would like to thank Editage (www.editage.cn) for English language editing.

Funding: This work was supported by the Research Fund of Shanghai Changning District Health Commission (No. 20234Y002 to L.L.).

Footnote

Reporting Checklist: The authors have completed the STROBE reporting checklist. Available at https://qims.amegroups.com/article/view/10.21037/qims-23-1730/rc

Conflicts of Interest: All authors have completed the ICMJE uniform disclosure form (available at https://qims.amegroups.com/article/view/10.21037/qims-23-1730/coif). L.L. reports a grant from the Research Fund of Shanghai Changning District Health Commission (No. 20234Y002) during the conduct of the study. The other authors have no conflicts of interest to declare.

Ethical Statement: The authors are accountable for all aspects of the work in ensuring that questions related to the accuracy or integrity of any part of the work are appropriately investigated and resolved. Ethical approval for this cross-sectional study with prospective data collection was obtained from the Institutional Review Board of Shanghai Tongren Hospital (No. 2022-044-01), and informed consent was obtained from the participants. The research reported in this article adhered to the guidelines of the Declaration of Helsinki (as revised in 2013).

References

1. van Middelkoop M, Bennell KL, Callaghan MJ, Collins NJ, Conaghan PG, Crossley KM, Eijkenboom JJFA, van der Heijden RA, Hinman RS, Hunter DJ, Meuffels DE, Mills K, Oei EHG, Runhaar J, Schiphof D, Stefanik JJ, Bierma-Zeinstra SMA. International patellofemoral osteoarthritis consortium: Consensus statement on the diagnosis, burden, outcome measures, prognosis, risk factors and treatment. Semin Arthritis Rheum 2018;47:666-75.
2. Duncan R, Peat G, Thomas E, Hay EM, Croft P. Incidence, progression and sequence of development of radiographic knee osteoarthritis in a symptomatic population. Ann Rheum Dis 2011;70:1944-8.
3. Crossley KM, Callaghan MJ, van Linschoten R. Patellofemoral pain. BMJ 2015;351:h3939.
4. Collins NJ, Oei EHG, de Kanter JL, Vicenzino B, Crossley KM. Prevalence of Radiographic and Magnetic Resonance Imaging Features of Patellofemoral Osteoarthritis in Young and Middle-Aged Adults With Persistent Patellofemoral Pain. Arthritis Care Res (Hoboken) 2019;71:1068-73.
5. Hart HF, Stefanik JJ, Wyndow N, Machotka Z, Crossley KM. The prevalence of radiographic and MRI-defined patellofemoral osteoarthritis and structural pathology: a systematic review and meta-analysis. Br J Sports Med 2017;51:1195-208.
6. Kobayashi S, Pappas E, Fransen M, Refshauge K, Simic M. The prevalence of patellofemoral osteoarthritis: a systematic review and meta-analysis. Osteoarthritis Cartilage 2016;24:1697-707.
7. Drew BT, Redmond AC, Smith TO, Penny F, Conaghan PG. Which patellofemoral joint imaging features are associated with patellofemoral pain? Systematic review and meta-analysis. Osteoarthritis Cartilage 2016;24:224-36.
8. Bohnsack M, Wilharm A, Hurschler C, Rühmann O, Stukenborg-Colsman C, Wirth CJ. Biomechanical and kinematic influences of a total infrapatellar fat pad resection on the knee. Am J Sports Med 2004;32:1873-80.
9. Zapata-Linares N, Eymard F, Berenbaum F, Houard X. Role of adipose tissues in osteoarthritis. Curr Opin Rheumatol 2021;33:84-93.
10. Li J, Zhu Z, Li Y, Cao P, Han W, Tang S, Li D, Kwoh CK, Guermazi A, Hunter DJ, Ding C. Qualitative and quantitative measures of prefemoral and quadriceps fat pads are associated with incident radiographic osteoarthritis: data from the Osteoarthritis Initiative. Osteoarthritis Cartilage 2020;28:453-61.
11. Widjajahakim R, Roux M, Jarraya M, Roemer FW, Neogi T, Lynch JA, Lewis CE, Torner JC, Felson DT, Guermazi A, Stefanik JJ. Relationship of Trochlear Morphology and Patellofemoral Joint Alignment to Superolateral Hoffa Fat Pad Edema on MR Images in Individuals with or at Risk for Osteoarthritis of the Knee: The MOST Study. Radiology 2017;284:806-14.
12. Kim JH, Lee SK. Superolateral Hoffa Fat Pad Edema and Patellofemoral Maltracking: Systematic Review and Meta-Analysis. AJR Am J Roentgenol 2020;215:545-58.
13. Erber B, Baur-Melnyk A, Glaser C, Goller S, Ricke J, Heuck A. Quadriceps fat pad edema in MR imaging: Association with quadriceps tendon alterations in a retrospective analysis. Eur J Radiol 2021;142:109858.
14. Tsavalas N, Karantanas AH. Suprapatellar fat-pad mass effect: MRI findings and correlation with anterior knee pain. AJR Am J Roentgenol 2013;200:W291-6.
15. Yasemin K, Ozum T. Anterior Knee Pain and Oedema-like Changes of the Suprapatellar Fat Pad: Correlation of the Symptoms with MRI Findings. Curr Med Imaging 2021;17:1350-5.
16. Yuksel Y, Ergun T, Torun E, Unal M, Sonnow L, Kose O. The relationship between quadriceps fat pad syndrome and patellofemoral morphology: a case-control study. J Orthop Traumatol 2021;22:17.
17. Erden A, Kuru Öz D, Peker E, Kul M, Özalp Ateş FS, Erden İ, İdilman R. MRI quantification techniques in fatty liver: the diagnostic performance of hepatic T1, T2, and stiffness measurements in relation to the proton density fat fraction. Diagn Interv Radiol 2021;27:7-14.
18. Chen Y, Zhang X, Li M, Zhong L, Ding Y, Zhang Y, Du X, Mo X, Chen J, Chen Q, Huang W, Zhong S, Zhang X. Quantitative MR evaluation of the infrapatellar fat pad for knee osteoarthritis: using proton density fat fraction and T2* relaxation based on DIXON. Eur Radiol 2022;32:4718-27.
19. Craig CL, Marshall AL, Sjöström M, Bauman AE, Booth ML, Ainsworth BE, Pratt M, Ekelund U, Yngve A, Sallis

JF, Oja P. International physical activity questionnaire: 12-country reliability and validity. Med Sci Sports Exerc 2003;35:1381-95.
20. Iwano T, Kurosawa H, Tokuyama H, Hoshikawa Y. Roentgenographic and clinical findings of patellofemoral osteoarthrosis. With special reference to its relationship to femorotibial osteoarthrosis and etiologic factors. Clin Orthop Relat Res 1990;(252):190-7.
21. Watson CJ, Propps M, Ratner J, Zeigler DL, Horton P, Smith SS. Reliability and responsiveness of the lower extremity functional scale and the anterior knee pain scale in patients with anterior knee pain. J Orthop Sports Phys Ther 2005;35:136-46.
22. Lee JH, Jang KM, Kim E, Rhim HC, Kim HD. Effects of Static and Dynamic Stretching With Strengthening Exercises in Patients With Patellofemoral Pain Who Have Inflexible Hamstrings: A Randomized Controlled Trial. Sports Health 2021;13:49-56.
23. Lee JH, Shin KH, Lee GB, Son S, Jang KM. Comparison of Functional Outcomes between Supervised Rehabilitation and Telerehabilitation in Female Patients with Patellofemoral Pain Syndrome during the COVID-19 Pandemic. Int J Environ Res Public Health 2023;20:2233.
24. Shah NS, Wang DM, Weinberg DS, Liu RW. Patellar Morphology and Osteoarthritis: A Cadaveric Analysis. J Knee Surg 2022;35:122-7.
25. Hunter DJ, Guermazi A, Lo GH, Grainger AJ, Conaghan PG, Boudreau RM, Roemer FW. Evolution of semi-quantitative whole joint assessment of knee OA: MOAKS (MRI Osteoarthritis Knee Score). Osteoarthritis Cartilage 2011;19:990-1002.
26. Yu K, Ying J, Zhao T, Lei L, Zhong L, Hu J, Zhou JW, Huang C, Zhang X. Prediction model for knee osteoarthritis using magnetic resonance-based radiomic features from the infrapatellar fat pad: data from the osteoarthritis initiative. Quant Imaging Med Surg 2023;13:352-69.
27. van der Heijden RA, de Kanter JL, Bierma-Zeinstra SM, Verhaar JA, van Veldhoven PL, Krestin GP, Oei EH, van Middelkoop M. Structural Abnormalities on Magnetic Resonance Imaging in Patients With Patellofemoral Pain: A Cross-sectional Case-Control Study. Am J Sports Med 2016;44:2339-46.
28. Cilengir AH, Cetinoglu YK, Kazimoglu C, Gelal MF, Mete BD, Elmali F, Tosun O. The relationship between patellar tilt and quadriceps patellar tendon angle with anatomical variations and pathologies of the knee joint. Eur J Radiol 2021;139:109719.
29. Patel J, Chen S, Katzmeyer T, Pei YA, Pei M. Sex-dependent variation in cartilage adaptation: from degeneration to regeneration. Biol Sex Differ 2023;14:17.
30. Macri EM, Neogi T, Jarraya M, Guermazi A, Roemer F, Lewis CE, Torner JC, Lynch JA, Tolstykh I, Jafarzadeh SR, Stefanik JJ. Magnetic Resonance Imaging-Defined Osteoarthritis Features and Anterior Knee Pain in Individuals With, or at Risk for, Knee Osteoarthritis: A Multicenter Study on Osteoarthritis. Arthritis Care Res (Hoboken) 2022;74:1533-40.
31. Collins NJ, Barton CJ, van Middelkoop M, Callaghan MJ, Rathleff MS, Vicenzino BT, Davis IS, Powers CM, Macri EM, Hart HF, de Oliveira Silva D, Crossley KM. 2018 Consensus statement on exercise therapy and physical interventions (orthoses, taping and manual therapy) to treat patellofemoral pain: recommendations from the 5th International Patellofemoral Pain Research Retreat, Gold Coast, Australia, 2017. Br J Sports Med 2018;52:1170-8.
32. Roth C, Jacobson J, Jamadar D, Caoili E, Morag Y, Housner J. Quadriceps fat pad signal intensity and enlargement on MRI: prevalence and associated findings. AJR Am J Roentgenol 2004;182:1383-7.
33. Collins NJ, Neogi T, Vicenzino B, Guermazi A, Roemer FW, Lewis CE, Torner JC, Nevitt MC, Stefanik JJ. Psychological and Pain Sensitization Characteristics Are Associated With Patellofemoral Osteoarthritis Symptoms: The Multicenter Osteoarthritis Study. J Rheumatol 2020;47:1696-703.
34. Sirvanci M, Ganiyusufoglu AK. Quadriceps fat pad signal intensity and enlargement on MRI. AJR Am J Roentgenol 2005;184:1708.
35. Jarraya M, Diaz LE, Roemer FW, Arndt WF, Goud AR, Guermazi A. MRI Findings Consistent with Peripatellar Fat Pad Impingement: How Much Related to Patellofemoral Maltracking? Magn Reson Med Sci 2018;17:195-202.
36. Biedert RM, Tscholl PM. Patella Alta: A Comprehensive Review of Current Knowledge. Am J Orthop (Belle Mead NJ) 2017;46:290-300.
37. Raju S, Chinnakkannu K, Balakumar B, Sundareyan R, Kaliappan SP, Puttaswamy MK. Different Patellar Indices and Their Role in Decision-Making: An MRI-Based Study. J Knee Surg 2021;34:853-8.
38. van Middelkoop M, Macri EM, Eijkenboom JF, van der Heijden RA, Crossley KM, Bierma-Zeinstra SMA, de Kanter JL, Oei EH, Collins NJ. Are Patellofemoral Joint Alignment and Shape Associated With Structural Magnetic Resonance Imaging Abnormalities and Symptoms Among

People With Patellofemoral Pain? Am J Sports Med 2018;46:3217-26.
39. Cosentino A, Richard R, Baron M, Demondion X, Favre J, Omoumi P. MRI signal and morphological alterations of the suprapatellar fat pad in asymptomatic subjects: are these normal variants? Skeletal Radiol 2022;51:1995-2007.
40. Tsai PH, Wong CC, Chan WP, Lu TW. The value of MR T2* measurements in normal and osteoarthritic knee cartilage: effects of age, sex, and location. Eur Radiol 2019;29:4514-22.
41. Haj-Mirzaian A, Guermazi A, Hafezi-Nejad N, Sereni C, Hakky M, Hunter DJ, Zikria B, Roemer FW, Demehri S. Superolateral Hoffa's fat pad (SHFP) oedema and patellar cartilage volume loss: quantitative analysis using longitudinal data from the Foundation for the National Institute of Health (FNIH) Osteoarthritis Biomarkers Consortium. Eur Radiol 2018;28:4134-45.
42. Can TS, Yilmaz BK, Özdemir S. Magnetic resonance imaging of the quadriceps fat pad oedema pattern in relation to patellofemoral joint pathologies. Pol J Radiol 2019;84:e375-80.
43. Fontanella CG, Belluzzi E, Rossato M, Olivotto E, Trisolino G, Ruggieri P, Rubini A, Porzionato A, Natali A, De Caro R, Vettor R, Ramonda R, Macchi V, Favero M. Quantitative MRI analysis of infrapatellar and suprapatellar fat pads in normal controls, moderate and end-stage osteoarthritis. Ann Anat 2019;221:108-14.

Cite this article as: Lyu L, Ren J, Lu W, Li Y, Zhong J, Yao W. Association between quadriceps fat pad edema and patellofemoral osteoarthritis: a quantitative Q-Dixon-based magnetic resonance imaging (MRI) analysis. Quant Imaging Med Surg 2024;14(5):3275-3288. doi: 10.21037/qims-23-1730

Appendix 1

Sample size

According to the preliminary experiment results (N=45):
For FF: AUC =0.8597 (95% CI, 0.750–0.969), Std.Error =0.05578, P<0.001.
For T2*: AUC =0.6858 (95% CI, 0.5302–0.8413), Std.Error =0.07937, P=0.0328.

The sample size is calculated by PASS (15.0) (N–/N+=0.5):

Tests for FF ROC curve

Numeric Results for Testing AUC = AUC0 with Continuous Data
FPR1 = 0. FPR2 = 1. B = 1.

Target Power	Actual Power	N+	N–	N	Target R	Actual R	AUC0'	AUC1'	Diff'	AUC0	AUC1	Diff	Alpha
0.9	0.92123	15	8	23	0.5	0.53333	0.5	0.8597	0.3597	0.5	0.8597	0.3597	0.05

Tests for T2* ROC Curve

Numeric Results for Testing AUC = AUC0 with Continuous Data
Test Type = Two-Sided. FPR1 = 0. FPR2 = 1. B = 1.

Target Power	Actual Power	N+	N–	N	Target R	Actual R	AUC0'	AUC1'	Diff'	AUC0	AUC1	Diff	Alpha
0.9	0.9015	69	35	104	0.5	0.50725	0.5	0.6858	0.1858	0.5	0.6858	0.1858	0.05

Finally, our sample size: N(PFOA) =80, N(no-PFOA) =40

https://dx.doi.org/10.21037/qims-23-1730